Thermal Conductivity Analysis of Graphene Oxide Nanofluid Using Three-Level Factorial Design

Munish Gupta, Jodh Singh, Harmesh Kumar, and Rajesh Kumar

Abstract Nanofluids improve the performance of thermal systems. Graphene oxide nanoparticles were characterized to confirm the structure, using X-ray diffraction and field-emission scanning electron microscopy. Water-based grapheme oxide nanofluids were synthesized. Three-level (3^2) factorial design was used to examine the effects changes in temperature and nanoparticle loading on the thermal conductivity of prepared nanofluids. Significance of model used was tested using analysis of variance at a 95.0% confidence interval. The results revealed that thermal conductivity varies directly with temperature as well as weight concentration. 30.4% thermal conductivity enhancement is observed at optimum conditions, i.e. high level of temperature (60 °C) and medium level of weight concentration (0.1 wt%).

Keywords Graphene oxide · Nanofluids · Heat transfer · Thermal conductivity · Factorial design

1 Introduction

The trend of miniaturization and increased heat loads in most of the industries call for the efficient heat transfer systems. Heat transfer depends mainly on thermal conductivity of the fluids. The thermal conductivity of generally used fluids, i.e., water, vegetable oil, engine oil, etc., can be improved by adding solid nanoparticles. Such two phase homogeneous mixtures of nanoparticles having size below 100 nm in conventional base fluids are known as nanofluids. Heat transfer occurs through conduction as well as convection. This leads to enhance heat transfer rate [1].

M. Gupta
Mechanical Engineering Department, GJUST, Hisar, Haryana, India

J. Singh (✉)
SSB University Institute of Chemical Engineering and Technology, Panjab University, Chandigarh, India
e-mail: jodhme@gmail.com

H. Kumar · R. Kumar
Mechanical Engineering Department, UIET, Panjab University, Chandigarh 160014, India

Table 1 Summary of literature on GO/water nanofluid

Nanofluid parameter	Range of parameters studied		Enhancement in thermal conductivity	References
	Concentration	Temperature (°C)		
GO/water	0.01–0.5 wt%	25–60	55.2% at 0.5% and 60 °C	[4]
GO/water	0.05–0.25 wt%	10–40	47.5% at 0.25% and 40 °C	[5]
r-GO/water	0.02–0.08 wt%	20–40	35.7% at 0.1% and 40 °C	[6]
GO/water	0.01–0.07 vol%	20–50	30% at 0.07% and 50 °C	[7]
GO/water	0.05–0.2 vol%	30–50	27% at 0.2 vol% and 50 °C	[8]

Graphene is consisting of single layer of carbon in two-dimensional lattice. It shows fascinating thermal properties because of larger surface area. Generally, oxide (GO) nanoparticles get dispersed in polar base fluids [2]. GO nanoparticles show higher thermal conductivity and long-term stability when dispersed in water. This is because of the hydrophilic nature and the presence of functional groups [3]. Therefore, GO and distilled water were selected for this work. Several studies are available on the heat transfer application of GO/water. Table 1 shows the summary of some experimental studies related to water-based GO nanofluids.

Studies witnessed the significant influence of temperature and nanoparticle loading on the thermal conductivity. There is an optimum value of particle concentration at specific temperature which maximizes thermal conductivity with minimum increase in viscosity [9]. Literature review shows that studies based on GO nanofluids using factorial design are not often found.

This paper discusses the effects of changes in temperature and nanoparticle loading on the thermal conductivity of GO/water nanofluids by using 3^2 factorial design.

2 Materials and Methods

Distilled water and GO nanoparticles were selected for preparing nanofluid samples. GO nanopowder was purchased from Nanoshel Company, Willmington, the USA. Specifications of GO as provided by supplier are given in Table 2. Specification and properties were further verified by characterizing nanoparticles.

Table 2 Composition of graphene oxide nanoparticles

Parameter	Purity	Layers	Thickness	Lateral dimensions	Surface area	Carbon	Oxygen	Others
Value	99%	1–3	1–4 nm	5–10 μm (X and Y)	200 m^2/g	77%	22%	1%
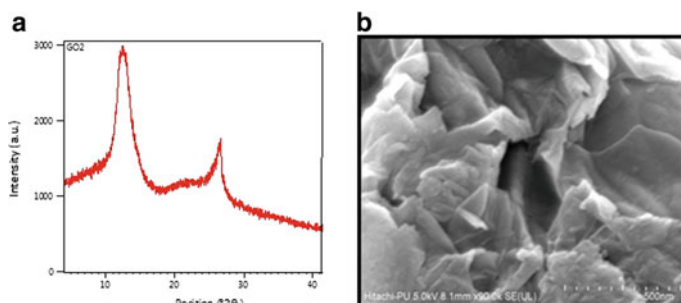
Fig. 1 **a** X-Ray diffraction result of GO, **b** FESEM result of GO

2.1 Characterization of Nanoparticles

XRD analysis of purchased powder was performed. One high-intensity (2900 a.u.) peak appeared at about 2θ value of 13 corresponding to (002) diffraction plane of graphite. XRD patterns are shown in Fig. 1a. Results confirmed the properties of GO. FESEM image in Fig. 1b showed the layers of graphene oxide surface. Size of sheets was in range of 5–10 μm. Nanosheets were tending to form multilayer clusters.

2.2 Synthesis of Nanofluids

Two-step method is generally used for oxide nanoparticles [10]. Three samples at 0.03, 0.1 and 0.3% weight concentration were prepared through this method by dispersing specified amount of GO nanoparticles in distilled water. Values of concentration levels were selected randomly on the basis of literature to examine the effects of low, medium and high concentration. Hydrophilic nature of GO shows good compatibility with water. So, no surfactant was used. Magnetic stirring of the samples was performed for two hours using the magnetic stirrer followed by ultrasonication for four hours in bath sonicator equipment. Stability was checked by sedimentation test. The prepared nanofluids were stable for ten days without any surfactant and after twelve days settled down completely.

Table 3 Design of experiment

Factors	Levels			Base runs	Replicate	Total runs	Blocks
	Low	Medium	High				
Temperature, A (°C)	30	45	60	9	2	18	2
Concentration, B (wt%)	0.03	0.1	0.3				

2.3 Factorial Design

Factorial design creates all possible experimental combinations for different factors at all the levels. Two factor three-level factorial (3^2) design was used in this work. Temperature and weight concentrations were selected as variable factors and thermal conductivity as response factor. To get the possible curve in response variable, three levels of each factor were considered. All the runs were randomly assigned in two blocks to distribute the error in the whole range of experiments. Table 3 shows the summary of the design. Total 18 runs at two replicates of nine experimental sets were performed as shown in Table 4.

2.4 Thermal Conductivity Measurement

KD2 Pro thermal analyzer (Decagon Devices, the USA) which is working on transient hot wire technique was used for the measurement. A water bath was used to get three different temperatures, i.e., 60, 45 and 60 °C, which were selected randomly. Samples were kept inside the bath after setting the required temperature. After getting the set temperature, samples were kept remained inside for further 10 min to achieve equilibrium. Then, each measurement was taken twice and recorded in Table 4. Measurements for distilled water were also performed at 30, 45 and 60 °C and found as 0.589, 0.618 and 0.625 W/mK, respectively.

3 Results and Discussion

Main and interaction effects of variable factors, i.e., temperature (A) and weight concentration (B) on response factor, i.e., thermal conductivity were studied through analysis of variance (ANOVA) by using MINITAB 19.

The results revealed that maximum value of thermal conductivity (0.95 W/mK) was found at high level of A and B, whereas minimum value (0.61 W/mK) was found at low level of A and B as shown in Table 3. Thus, 3.6–52% thermal conductivity enhancement was recorded when compared to distilled water at the same

Table 4 Factorial design layout

Standard order	Run order	Blocks	Temperature, A (°C)	Concentration, B (wt%)	Thermal conductivity (W/mK)
3	1	1	30	0.30	0.891
5	2	1	45	0.10	0.781
6	3	1	45	0.30	0.910
8	4	1	60	0.10	0.820
1	5	1	30	0.03	0.610
4	6	1	45	0.03	0.701
7	7	1	60	0.03	0.741
9	8	1	60	0.30	0.950
2	9	1	30	0.10	0.690
13	10	2	45	0.03	0.692
12	11	2	30	0.30	0.870
16	12	2	60	0.03	0.746
15	13	2	45	0.30	0.918
18	14	2	60	0.30	0.946
14	15	2	45	0.10	0.782
17	16	2	60	0.10	0.810
11	17	2	30	0.10	0.700
10	18	2	30	0.03	0.622

conditions. In Pareto chart A, B and $A * B$ extended the reference line which shows that main effects and interactive effects of the factors are significant for response factor. Figure 2b shows that response factor varies directly with temperature and concentration of particles. The interaction effects of A and B are shown in Fig. 2c. If some points are away from the fitted line, this indicates that effects are real and important as well [11]. Figure 2d shows that some points are away from fitted line. This indicates the reality and importance of effects. Points in residuals plots followed a straight line. Such results indicate the normality of the data and error distribution.

3.1 Analysis of Variance

In this analysis, significance and fitness of the present model were checked. Large F-value, small P-value and value of R square (R^2) near 100% indicates a good fit model and ensures validity of model [12]. Results are shown in Table 5.

P-value is zero for both factors A and B. This indicates that A and B are significant for response factor, i.e., thermal conductivity. However, F-value for factor A and B was 281.04 and 1345.27, respectively. Small P-values and high F-values indicate that
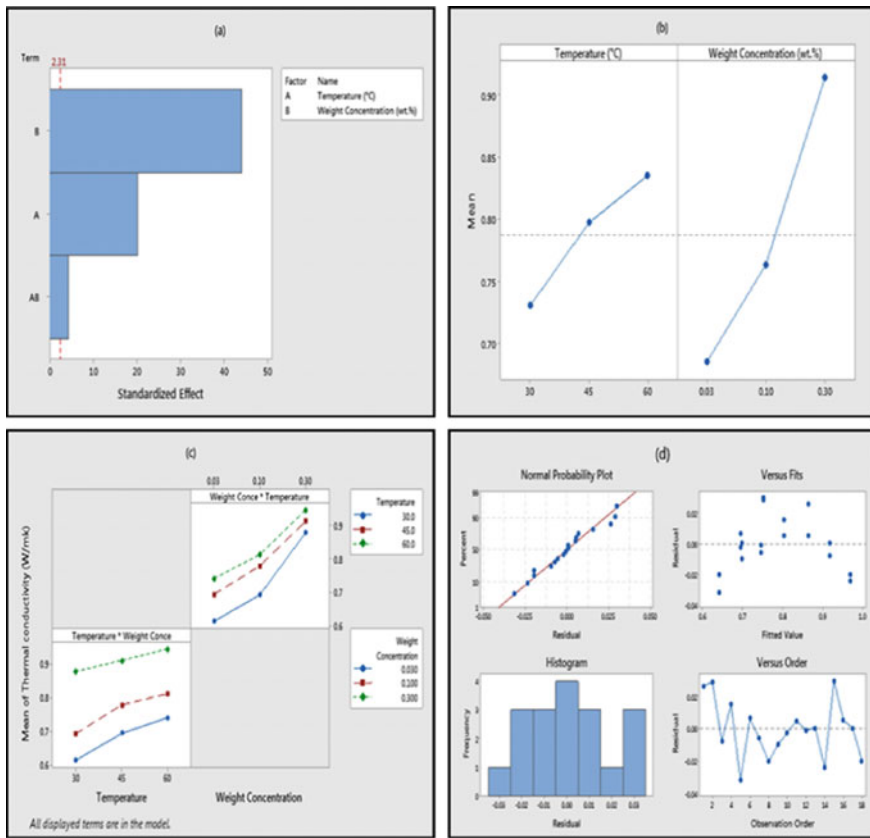
Fig. 2 **a** Pareto chart, **b** main effects, **c** interactive effects, **d** residual plots

present model is a valid model. Values of different R square are shown in Table 5. High value of R square (99.76%) proves this model being a good fit model. This indicates that the model is capable of responding to 99.7% variability in response factor. High value of adjusted R square (99.49%) indicates that the model is most significant. The least difference between R^2 and adjusted R^2 indicates the absence of any insignificant factor [13]. All the values of R^2 are close to each other. This proves that selected factors are very significant.

3.2 Response Optimization and Proposed Equation

The goal is to maximize thermal conductivity with low value of 0.61 W/mK and target value of 0.95 W/mK. The fit optimum value for thermal conductivity predicted by design software, based on the present model, is 0.815 W/mK with 95% confidence

Table 5 ANOVA table

Source	Degree of freedom	Adjusted sum of squares	Adjusted mean sum of squares	*F*-Value	*P*-Value	Significance
Model	9	0.198781	0.022087	366.25	0.000	Significant
Blocks	1	0.000004	0.000004	0.06	0.814	Not significant
Linear	4	0.196151	0.049038	813.15	0.000	Significant
A	2	0.033897	0.016948	281.04	0.000	Significant
B	2	0.162254	0.081127	1345.27	0.000	Significant
Two way interaction	4	0.002626	0.000657	10.89	0.003	Significant
A * *B*	4	0.002626	0.000657	10.89	0.003	Significant
Error	8	0.000482	0.000060			
Total	17	0.199263				
R^2	99.76%					
Adj. R^2	99.49%					
Pred. R^2	98.77%					

interval which is near to actual experimental values, i.e., 0.81 and 0.82. Optimum thermal conductivity (0.815 W/mK) with 30.4% enhancement was observed at high level of *A* (60 °C) and medium level of *B* (0.1 wt%).

Through this ANOVA-based factorial design, the following equation regarding the variable factors, i.e., *A* and *B*, is proposed for the prediction of thermal conductivity (*k*).

$$k = 0.5118 + 0.003500 * A + 0.8264 * B \tag{1}$$

The model values show good correspondence between actual and predicted data. Figure 2d shows the plots for residuals (difference between actual and fitted values) which show the normal error distribution and no specific pattern of the residuals. This also confirms the compatibility of actual and predicted values of thermal conductivity.

3.3 Contour and Surface Plots

The contour plots show the relationship between a fitted response, i.e., thermal conductivity and variable factors, i.e., *A* and *B*. Surface plots give three-dimensional view of the surfaces, generated by connecting the points that have same response. These plots give the information regarding the trend and pattern of effects of different factors on the thermal conductivity. Figure 3a, b indicates that both parameters show significant influence on response factor. With rise in variable factors, thermal
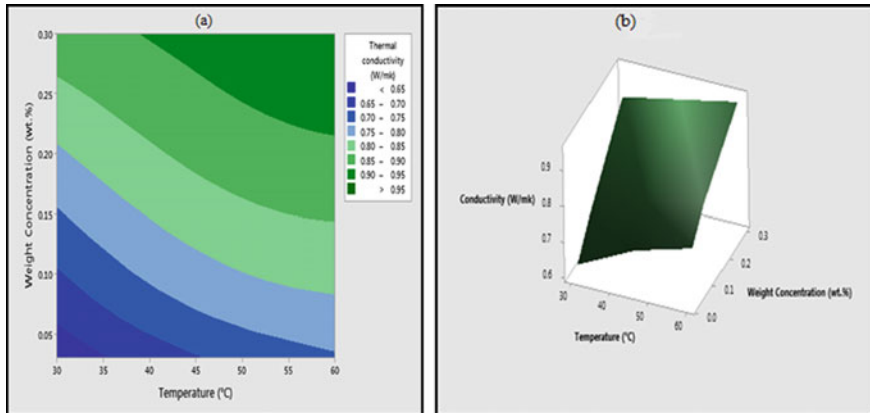
Fig. 3 a Contour plots, **b** surface plot for interactive effects of factors

conductivity shows rising trend. Thermal conductivity shows linear relationship with temperature. Significance of this trend increases toward higher side of weight concentration. Trends of these plots were in compliance with values of Table 3. The highest and the lowest thermal conductivity were obtained, respectively, at high and low level of *A* and *B*. This indicates the linear relationship of thermal conductivity with temperature (*A*) as well as weight concentration of particles (*B*). This linear trend may be due to increase in the number of particles as well as collisions among them at high concentration and high temperature.

4 Conclusion

The prepared nanofluids were stable for ten days without any surfactant. The maximum thermal conductivity (0.95 W/mK) was found at high level of temperature (60 °C) and weight concentration of nanoparticles (0.3 wt%), whereas the minimum value (0.61 W/mK) was found at low level of both factors, i.e., 30 °C and 0.03 wt%. Thus, total enhancement in thermal conductivity using nanofluid varies from 3.6 to 52%. The study confirms that the addition of nano-sized GO particles in water enhances its thermal conductivity.

Main effects as well as interactive effect of temperature and weight concentration were significant in affecting the thermal conductivity. It is confirmed that temperature and weight concentration show linear relation with thermal conductivity.

Optimum thermal conductivity (0.815 W/mK) was found at high level of temperature (60 °C) and medium level of weight concentration (0.1 wt%).

References

1. Fuskele, V., & Sarviya, R. M. (2017). Recent developments in nanoparticles synthesis, preparation and stability of nanofluids. *Materials Today: Proceedings, 4*(2), 4049–4060.
2. Mukherjee, S. (2013). Preparation and stability of nanofluids—A review. *IOSR Journal of Mechanical and Civil Engineering, 9*(2), 63–69. https://doi.org/10.9790/1684-0926369.
3. Hu, X., Yu, Y., Zhou, J., & Song, L. (2014). Effect of graphite precursor on oxidation degree, hydrophilicity and microstructure of graphene oxide. *Nano, 9*(03), 1–8.
4. Esfahani, M. R., Languri, E. M., & Nunna, M. R. (2016). Effect of particle size and viscosity on thermal conductivity enhancement of graphene oxide nanofluid. *International Communications in Heat and Mass Transfer, 76,* 308–315.
5. Hajjar, Z., Morad Rashidi, A., & Ghozatloo, A. (2014). Enhanced thermal conductivities of graphene oxide nanofluids. *International Communications in Heat and Mass Transfer, 57,* 128–131.
6. Sadri, R., Zangeneh Kamali, K., Hosseini, M., Zubir, N., Kazi, S. N., Ahmadi, G., et al. (2017). Experimental study on thermo-physical and rheological properties of stable and green reduced graphene oxide nanofluids: Hydrothermal assisted technique. *Journal of Dispersion Science and Technology, 38*(9), 1302–1310.
7. Hadadian, M., Goharshadi, E. K., & Youssefi, A. (2014). Electrical conductivity, thermal conductivity, and rheological properties of grapheme oxide based nanofluids. *Journal of Nanoparticle Research, 16*(12), 2788. https://doi.org/10.1007/s11051-014-2788-1.
8. Sen Gupta, S., Manoj Siva, V., Krishnan, S., Sreeprasad, T. S., Singh, P. K., Pradeep, T., et al. (2011). Thermal conductivity enhancement of nanofluids containing graphene nanosheets. *Journal of Applied Physics, 110*(8), 084302. https://doi.org/10.1063/1.3650456.
9. Yanuar, N. P., & Gunawan, M. B. (2011). Flow and Convective heat transfer characteristics of spiral pipe for nanoparticles. *International Journal of Research and Reviews in Applied Sciences, 7*(3), 236–248.
10. Pal, S. L., Jana, U., Manna, P. K., Mohanta, G. P., & Manavalan, R. (2011). Nanoparticle: An overview of preparation and characterization. *Journal of Applied Pharmaceutical Science, 1*(6), 228–234.
11. Plackett, R. L., & Burman, J. P. (1946). The design of optimum multi factorial experiments. *Biometrika, 34,* 255–272.
12. Pramanik, A., Islam, M. N., Basak, A. K., Dong, Y., Littlefair, G., & Prakash, C. (2019). Optimizing dimensional accuracy of titanium alloy features produced by wire electrical discharge machining. *Materials and Manufacturing Processes*, *34*(10), 1083–1090.
13. Prakash, C., Singh, S., Singh, M., Antil, P., Aliyu, A. A. A., Abdul-Rani, A. M., & Sidhu, S. S. (2018). Multi-objective Optimization of MWCNT Mixed Electric Discharge Machining of Al–30SiC p MMC Using Particle Swarm Optimization. In *Futuristic Composites* (pp. 145–164). Singapore: Springer.